WILEY-BLACKWELL

Cladistics (2013) 1–14

Cladistics

10.1111/cla.12021

Phylogenetic relationships of *Hamadryas* (Nymphalidae: Biblidinae) based on the combined analysis of morphological and molecular data

Ivonne J. Garzón-Orduña[a,*], Onildo Marini-Filho[b], Steve G. Johnson[a] and Carla M. Penz[a]

[a]*2000 Lakeshore Drive, Department of Biological Sciences, University of New Orleans, New Orleans, LA, 70148, USA;* [b]*Centro Nacional de Pesquisa e Conservação da Biodiversidade do Cerrado e da Caatinga—CECAT, Instituto Chico Mendes de Conservação da Biodiversidade—ICMBio, Brasília, DF, Brazil*

Accepted 25 January 2013

Abstract

A new phylogenetic hypothesis for the Neotropical butterfly genus *Hamadryas*, based on the combination of a morphological matrix, one mitochondrial (COI) and four nuclear markers (CAD, RpS5, EF1a, and Wingless), is presented. Results from analyses of the molecular evidence are compared with a previously published morphological phylogeny. Molecular data and the analysis of the complete dataset support the monophyly of *Hamadryas* and most sister groups suggested by morphological data alone. The addition of DNA sequences to the morphological matrix helped define species groups for which no morphological synapomorphies were found. Partitioned Bremer support indicates that COI, CAD, and morphology were consistently in agreement with the combined evidence tree. In contrast, signal from the nuclear markers Rps5, EF1a, and Wingless showed indifference at most levels of the tree, and minor conflict at nodes solving the relationships between species groups. Though resolved, the combined evidence tree shows low resample values, particularly among species groups whose relationships were characterized by short internodes. A reassessment about the pattern of character change for sound production is presented and discussed.

Introduction

Hamadryas is one of the most popular and easily recognized groups of Neotropical butterflies (Fruhstorfer, 1916; DeVries, 1987). The genus includes widespread species such as *H. feronia* and *H. amphinome*, which occupy a wide variety of habitats (Muyshondt and Muyshondt, 1975a,b). These species are also noticable due to the ability of males to produce audible sound while in flight (Godman and Salvin, 1883). Sound is produced in two ways: by contact between swollen veins located at the distal edge of the forewing discal cell (Fig. 1) at the end of the upstroke (Otero, 1990), or by deformation of a particular region of the forewing, in which case each wing produces sound independently (Yack et al., 2000). Eight of the 20 species in the genus have this particular venation, and it is believed that these are the only species capable of producing sound (Marini-Filho and Benson, 2010; Garzón-Orduña, 2012). Field observations (Otero, 1988; Yack et al., 2000) and cage experiments (Marini-Filho and Benson, 2010) suggested that sound is used as a mechanism for sexual recognition.

The two most important contributions to the systematics of this genus used complementary approaches. The taxonomic revision by Jenkins (1983) revived the use of the name *Hamadryas* (in the past, species in *Hamadryas* were segregated in four genera, see Garzón-Orduña, 2012 for a historical overview) and restructured species definitions by synonymizing nearly 100 names (recognizing only 20 species, see also

*Corresponding author.
E-mail address: ivonne.garzon@gmail.com

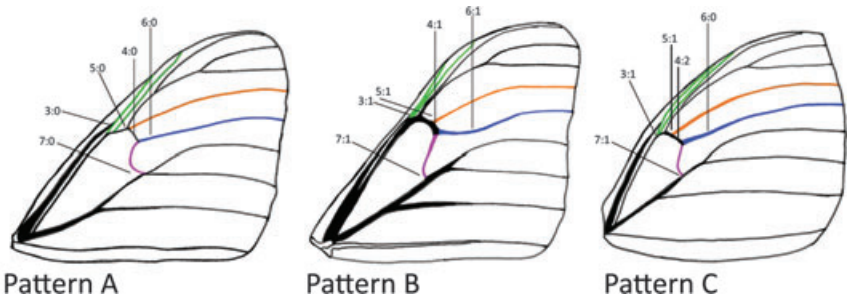

Fig. 1. Schematic venation patterns present in *Hamadryas* featuring in different colours the five characters associated with sound production. Pattern A corresponds to the venation of species that do not produce sound and pattern B to the venation of species that produce sound; pattern C is the venation present in *H. laodamia*, *H. velutina*, and *H. arete* (the latter not included in this study).

Lamas, 2004) and suggested the existence of three subgenera. Based on this taxonomic framework, Garzón-Orduña (2012) presented the first phylogenetic hypothesis for *Hamadryas* using 93 characters mostly from genitalia and wing colour (Fig. 2). The phylogeny was used to test whether the subgenera recognized by Jenkins (1983) constituted natural groups, and to study the pattern of character changes in sound production and sexual dimorphism. Morphology supported the monophyly of *Hamadryas*, and only one of the previously suggested subgenera was found to be monophyletic (the clade composed of *H. laodamia*, *H. arete*, and *H. velutina*; Fig. 2). The optimization of sound production, sexual dimorphism, and presence of androconial scales onto the phylogeny produced important inferences about the evolution of male–male and male–female interactions. Garzón-Orduña (2012) showed that male sound production is a derived condition that evolved once and was lost once in *Hamadryas*, and that this loss was congruent with the evolution of sexual dimorphism and androconial scales (Fig. 2). It was concluded from this study that these associated changes implied a shift in the main signal used for sexual recognition from acoustic to visual plus chemical cues.

The advantages of including multiple, independent sources of data in phylogenetic studies are widely acknowledged (Gatesy et al., 1999; Baker and Gatesy, 2002; Wahlberg et al., 2005). For example, Wahlberg and Nylin (2003) were able to resolve conflicting rela-

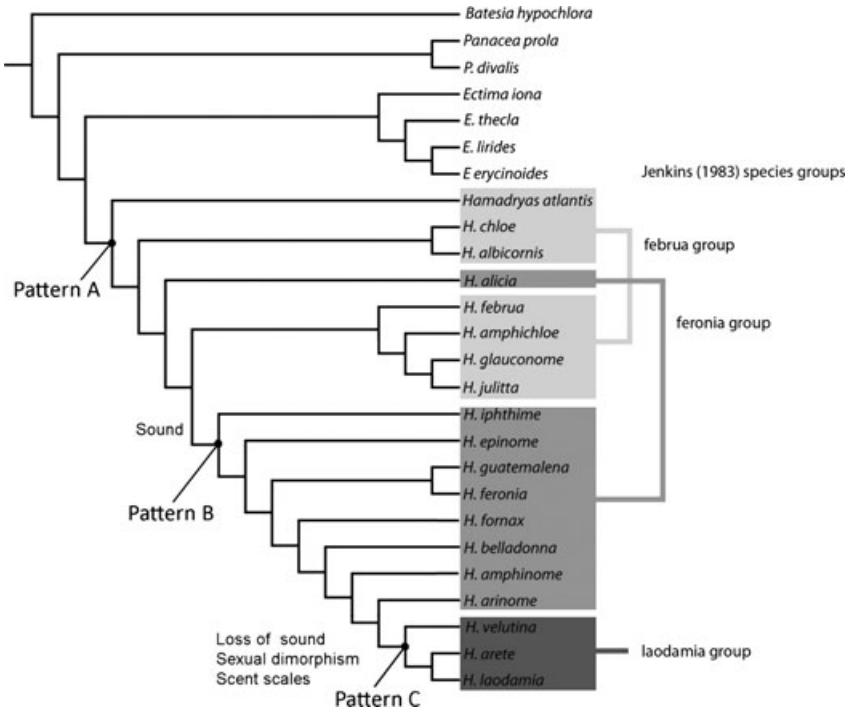

Fig. 2. Phylogeny of *Hamadryas* based on 93 morphological characters from Garzón-Orduña (2012) with venation patterns optimized on the tree. Origin and loss of sound production, sexual dimorphism, and androconial scales are labelled at the corresponding branches. Previously suggested species groups are highlighted in grey.

tionships among species of *Polygonia* by adding sequence data for two genes (mitochondrial COI and nuclear Ef1a) to a previous matrix (Nylin et al., 2001) that combined morphology and sequence data for two other genes (mitochondrial ND1 and nuclear Wingless). Furthermore, relationships based on the larger dataset had higher support than the previous hypothesis. Their findings are in agreement with other studies that used either parsimony or model-based analyses and spanned various taxonomic levels (Miller et al., 1997; Giannini and Simmons, 2005; Lopardo et al., 2011).

The main advantage of combining characters from different sources in a simultaneous analysis relies on the power of their congruence, given that there is only one tree of life (Kluge, 1989; Gatesy et al., 1999). Phylogenetic signal is expected to increase with the addition of characters, overriding the potential misleading effect of stochastic noise or homoplasy. Furthermore, because the support of a group depends on the amount of evidence favouring it relative to the amount of evidence against it, the interaction between characters is a decisive factor in estimating the degree of support (Goloboff et al., 2003). The inclusion of as much evidence as possible is therefore an effective approach to estimate the reliability of novel or traditionally accepted groups. The use of measurements of character conflict does not oppose the combination of all the evidence (Kluge, 1989) as they are used not to exclude incongruent data, but to identify the source of conflicting signals such as the incongruence length difference test (ILD), Mickevich and Farris (1981), Farris et al. (1994a) and partitioned Bremer support (PBS), Baker and DeSalle (1997). Although the previously proposed morphology-based phylogeny for *Hamadryas* was well resolved (Garzón-Orduña, 2012; Fig. 2) and the topology was resilient to different values of the concavity constant under implied weights, several nodes had low support, implying ambiguity. Thus phylogenetic studies of this genus benefit from consideration of additional data.

This study provides a phylogeny for *Hamadryas* using multiple independent data sources. New DNA sequence data (one mitochondrial and four nuclear markers) were added to a morphological matrix from Garzón-Orduña (2012), and the analyses aim to compare the phylogenetic signal provided by molecular and morphological data, as well as to revise previous inferences about the evolution of sound production based on the combination of both character systems.

Materials and methods

Specimens

This study used field collected and preserved specimens from museum or personal collections. The samples were either conserved in 96–100% ethanol or dried. A total of 40 specimens representing 17 of the 20 species of *Hamadryas* were sequenced. Sequences of five outgroup species were obtained from GenBank (http://www.ncbi.nlm.nih.gov/genbank). Table 1 lists the collection locality and GenBank accession number for all specimens.

Gene selection

One mitochondrial (*Cytochrome oxidase subunit I*, COI) and four nuclear genes (*Ribosomal protein S5*, RpS5; *Carbamoylphosphate synthase domain protein*, CAD; *Wingless*, WG; *Elongation factor 1α*, EF1a) were selected for this study. These markers were chosen because they are highly variable (Wahlberg and Wheat, 2008) and were phylogenetically informative at the species level for several butterfly groups (Jiggins et al., 2006; Silva Brandão et al., 2008; Penz et al., 2012). Table 2 lists the primers used and their sources.

DNA extraction and sequencing

One or two legs from each specimen were used for DNA extraction. Genomic DNA was extracted using the DNeasy Tissue Kit (Qiagen, Valencia, CA, USA). Gene amplification followed a standard polymerase chain reaction (PCR). PCRs were in a 20 μL volume and included 1 μL DNA extract. The master mix initially contained, per sample: 12.5 μL dH_2O, 2 μL 10× buffer, 2 μL $MgCl_2$, 1 μL forward primer, 1 μL reverse primer, 0.4 μL dNTP, 0.1 μL Taq polymerase, and 1 μL of the DNA extract, following the protocols published in Wahlberg and Wheat (2008); in the final stages of the study, the master mix contained 12.5 μL of OneTaq™ 2× MM (New England Biolabs, Ipswich, MA, USA), 0.5 μL forward primer, 0.5 μL reverse primer, and 5.5 μL water per sample. The general thermocycler profile included: denaturation at 95 °C for 5 min, followed by 40 cycles of 94 °C for 30 s, 50 °C for 30 s (annealing temperature, see below), 72 °C for 1 min 30 s, and a final extension at 72 °C for 10 min. To obtain a single band of the targeted PCR product, the annealing temperature was adjusted depending on the primer used (nuclear primers required higher temperatures) and the quality of DNA.

PCR products were purified with ExoSAP-IT (usb®). The master mix for the sequencing reaction included per sample 1 μL BigDye® Terminator v. 3.1 (Applied Biosystems), 1.5 μL BigDye® Terminator 5× sequencing buffer, 3 μL water, and 1.5 μL of the primer. Sequencing was conducted in both directions (forward and reverse) for all samples. The sequencing reaction included 3 μL of the purified PCR product and 7 μL of the sequencing reaction master mix. Sequencing was carried out on an ABI 3130 XL

Table 1
Specimens used for molecular analysis, numbers with locality and GenBank accession numbers

Species name	Voucher code	CAD	COI	EF1-Alpha	RPS5	WG	Locality
Hamadryas amphinome	JLBMEX01	KC494890	KC541620	KC541582	KC561474	KC541659	El Azulillo, Candelaria Loxicha, Oaxaca. México
H. amphinome	UJCUN017	KC494907	KC541638	KC541599	KC561491	KC541675	Puerto Bogotá, Cundinamarca, Colombia
H. amphinome	PD0914	KC494895	KC541625	KC541587	KC561479	KC541664	Madre de Dios, Los Amigos Research Center, Perú
H. amphinome	PD0915	KC494896*	KC541626*	KC541588	KC561480	KC541665	Madre de Dios, Los Amigos Research Center, Perú
H. amphinome	UFL01669	KC494902	KC541632	KC541594	KC561486	KC541671	Ecuador
H. arinome	IGLS66	KC494880	KC541610	KC541572	KC561464	KC541649	La Selva Biological Station, Heredia, Prov., Costa Rica
H. arinome	PURPER55	KC494898	KC541628	KC541590	KC561482	KC541667	Tingo Maria, Perú
H. arinome	PD0917	KC494897	KC541627	KC541589*	KC561481	KC541666	Madre de Dios, Los Amigos Research Center, Perú
H. arinome	UJAMZ011	KC494905	KC541636	KC541597	KC561489	KC541674	Leticia, Amazonas, Colombia
H. alicia	UJ88		KC541634*				San Martin de Amacayacú, Puerto Nariño, Colombia
H. amphichloe	DC027	KC494876	KC541606	KC541568	KC561460	KC541645	Chicamocha River, Santander, Colombia
H. amphichloe	DC028	KC494877	KC541607	KC541569	KC561461	KC541646	Suarez River, Santander, Colombia
H. amphichloe	BPAMPHC01	KC494875	KC541605*	KC541567	KC561459	KC541644	Pedernales, Dominican Republic
H. atlantis	ADW24	KC494872	KC541602	KC541564	KC561456	KC541641	Oaxaca, Mexico
H. belladonna	UJAMZ012	KC494906	KC541637*	KC541598	KC561490		Leticia, Amazonas, Colombia
H. chloe	IGMET001	KC494881	KC541611	KC541573	KC561465	KC541650	Villavicencio, Meta, Colombia
H. chloe	IGMET002	KC494882	KC541612	KC541574	KC561466	KC541651	Villavicencio, Meta, Colombia
H. epinome	MVHI	KC494893	KC541623	KC541585	KC561477	KC541662	Florianópolis, Mata Atlantica, Brazil
H. februa	NW62-3	EU141324	AY090216	AY090182	EU141402	AY090149	
H. februa	MVH60	KC494892	KC541622*	KC541584	KC561476	KC541661	Florianópolis, Mata Atlantica, Brazil
H. feronia	UFL01662	KC494900*	KC541630	KC541592*	KC561484	KC541669	Ecuador
H. feronia	UFL01663	KC494901	KC541631	KC541593	KC561485	KC541670	Ecuador
H. feronia	MH026	KC494891	KC541621	KC541583	KC561475	KC541660	Capurganá, Choco, Colombia
H. feronia	DC029	KC494878	KC541608	KC541570	KC561462	KC541647	Suarez River, Santander, Colombia
H. fornax	IGBUC30	KC494879	KC541609	KC541571*	KC561463	KC541648	Bucaramanga, Santander, Colombia
H. fornax	IGMET004	KC494884	KC541614	KC541576*	KC561468	KC541653	Villavicencio, Meta, Colombia
H. fornax	IGMET008	KC494886	KC541616	KC541578*	KC561470	KC541655	Villavicencio, Meta, Colombia
H. glauconome	ADW04	KC494871	KC541601	KC541563	KC561455	KC541640	Starrco. Rio Grande City, Fort Ringold, Texas, USA
H. glauconome	IGPV73	KC494887	KC541617	KC541579	KC561471	KC541656	Palo Verde Biological Station, Guanacaste, Costa Rica
H. glauconome	IGPV82	KC494889	KC541619	KC541581	KC561473	KC541658	Palo Verde Biological Station, Guanacaste, Costa Rica
H. guatemalena	IGPV74	KC494888	KC541618	KC541580	KC561472	KC541657	Palo Verde Biological Station, Guanacaste, Costa Rica
H. guatemalena	PURSALVA45	KC494899	KC541629	KC541591*	KC561483	KC541668	Ahuachapan, El Salvador
H. guatemalena	ADW02	KC494870	KC541600	KC541562	KC561454	KC541639	Starrco. Rio Grande City, Fort Ringold, Texas, US
H. iphthime	UJ90	KC494904	KC541635	KC541596*	KC561488	KC541673	Puerto Bogota, Cundinamarca, Colombia
H. julitta	ADW25	KC494873	KC541603	KC541565	KC561457	KC541642	Mexico, Campeche, Nadzcaan
H. julitta	ADW26	KC494874	KC541604	KC541566	KC561458	KC541643	Mexico, Campeche, Nadzcaan
H. laodamia	PD0913	KC494894	KC541624	KC541586	KC561478	KC541663	Madre de Dios, Los Amigos Research Center, Perú
H. laodamia	IGMET003	KC494883	KC541613	KC541575	KC561467	KC541652	Villavicencio, Meta, Colombia
H. laodamia	IGMET005	KC494885	KC541615	KC541577	KC561469	KC541654	Villavicencio, Meta, Colombia
H. velutina	UJ015	KC494903	KC541633*	KC541595	KC561487	KC541672*	Puerto Bogotá, Cundinamarca, Colombia

Table 1
(Continued)

Species name	Voucher code	CAD	COI	EF1-Alpha	RPS5	WG	Locality
Out-groups							
Ectima thecla	NW114-3	GQ864643	GQ864762	GQ864856	GQ865429	GQ864451	
Batesia hypochlora	NW109-5	GQ864619	GQ864743	GQ864837	GQ865402	GQ864431	
Panacea regina	NW109-8	GQ864691	AY788600	AY788702	GQ865480	AY788464	
Eunica viola	NW93-12	NA	GQ864767	GQ864861	NA	GQ864455	
Sevenia boisduvali	NW88-15	GQ864710	AY218247	AY218267	GQ865495	AY218285	
Length of marker (bp)		850	1470	1240	613	403	4576

*Incomplete fragment.

Table 2
Primers used for PCR and sequencing reactions and their sources

Marker	Sequence	Source
COI		
LCO (f)	G GTC AAC AAA TCA TAA AGA TAT TGG	Folmer et al. (1994)
HCO (r)	T AAA CTT CAG GGT GAC CAA AAA ATC A	Folmer et al. (1994)
Jerry (f)	C AAC AYT TAT TTT GAT TTT TTG G	Simon et al. (1994)
Pat (r)	A TCC ATT ACA TAT AAT CTG CCA TA	Simon et al. (1994)
Wingless		
LepG1 (f)	G ART GYA ART GYC AYG GYA TGT CTG G	Brower and DeSalle (1998)
LepG2 (r)	A CTI CGC ARC ACC ART GGA ATG TRC A	Brower and DeSalle (1998)
Rps5		
HybrpS5degF	A TGG CNG ARG ARA AYT GGA AYG A	Wahlberg and Wheat (2008)
HybrpS5degR	C GGT TRG AYT TRG CAA CAC G	Wahlberg and Wheat (2008)
CAD		
CAD743nF	G GNG TNA CNA CNG CNT GYT TYG ARC C	Wahlberg and Wheat (2008)
CADmidR	C ATT CWG CKG CWA CTG TAT C	Wahlberg and Wheat (2008)
CADmidF	K GGA TTY TCN GAY AAA CAA ATN GC	Wahlberg and Wheat (2008)
CAD1028R	T TRT TNG GNA RYT GNC CNC CCA T	Wahlberg and Wheat (2008)
EF1-alpha		
Starsky	C ACA TYA ACA TTG TCG TSA TYG G	Cho et al. (1995)
Monica	C ATR TTG TCK CCG TGC CAr CC	Cho et al. (1995)
HybAlF	G AGG AAA TYA ARA ArG AAG	Cho et al. (1995)
HybEFrcM4	A CAG CVA CKG TYT GYC TCA TRT C	Cho et al. (1995)

Genetic Analyzer (Applied Biosystems) at the University of New Orleans.

Sequence edition and alignment

Chromatogram evaluation, editing, and assembly were conducted using Geneious 5 (Drummond et al., 2011). All sequences were subjected to a search in BLAST (implemented by the National Center for biotechnology Information (NCBI) website http://www.ncbi.nlm.nih.gov) against the GenBank nucleotide database to test for contamination and to confirm the targeted marker. SequenceMatrix 1.78 (Vaidya et al., 2011) was used to check for unexpected identical sequences within genes. Heterozygous positions (those with two peaks of the same height) in the nuclear genes were coded following the International Union of Pure and Applied Chemistry (IUPAC) ambiguity code. Gene partitions were aligned in MUSCLE (Edgar, 2004) from Geneious under default settings, and the alignment did not contain gaps.

Phylogenetic analysis

A previously published morphological matrix (Garzón-Orduña, 2012) was modified to include *Panacea regina* and to exclude taxa for which molecular sequences were not available. Excluded taxa were: *Ectima erycinoides*, *E. lyrides*, *E. iona*, *Panacea divalis*, *P. prola* (all outgroups), *Hamadryas albicornis*, and *H. arete*. *Hamadryas rosandra* was not available for either morphological or molecular studies. The morphological matrix (hereafter morphology partition) and DNA sequences from the five molecular markers (hereafter molecular partition) were concatenated using SequenceMatrix 1.78 (Vaidya et al., 2011), and

the combined matrix was exported as TNT (Goloboff et al., 2008), Phylip and Nexus formats. In the combined matrix, morphological character states were repeated for multiple samples of the same species.

The combined matrix includes 93 characters from morphology (85 informative), and 4576 bp from DNA sequence (878 informative). The matrix was analysed under parsimony in TNT (Goloboff et al., 2008), Bayesian inference (BI) in MrBayes v. 3.1.2 (Huelsenbeck and Ronquist, 2001), and maximum likelihood (ML) in RaxML (Stamatakis et al., 2008). All characters were unordered. Exploratory analyses of individual genes (or gene partitions) were conducted to examine resolution levels and to determine which nodes were consistently recovered. Nonetheless, results from analyses of the complete dataset are favoured because this increases explanatory power, maximizes character independence, and allows the emergence of secondary signal or hidden support (Kluge, 1989; Nixon and Carpenter, 1996; Baker and DeSalle, 1997).

Parsimony analyses explored equal weights (EW) and extended implied weights (EIW), which aimed at minimizing the effect of homoplasy over phylogenetic signal (command xpiwe). Under this command, character sets (e.g. genes) are weighted using their average homoplasy (P. Goloboff, pers. comm.). Additionally, because characters with missing entries cannot have as much homoplasy as observed characters (and therefore would receive a high fit), the option piwe(* was included in the EIW analysis to determine the weights based on the number of missing entries present in the set (P. Goloboff, pers. comm.). Under EIW, many values of the concavity constant were explored, k = 1–50. Parsimony searches included 500 replicates of random addition sequence holding 10 trees per replication, tree bisection and reconnection (TBR) for branch swapping, and 90 iterations of Ratchet (Nixon, 1999) (mult: replic 500 tbr hold 10 ratchet). After the search, zero-length branches were collapsed and duplicate trees discarded (coll rule 4; condense; unique).

Bayesian and ML searches used GTR + Γ as the model of molecular substitutions. The Akaike information criterion (AIC) in jModelTest 2 (Darriba et al., 2012) was used to select the model and model parameters for Bayesian analysis. RaxML uses the GTR + Γ model by default (RaxML Manual: http://sco.h-its.org/exelixis/oldPage/RAxML-Manual.7.0.4.pdf). The morphological partition was analysed under the "standard discrete model" (Lewis, 2001). State frequencies and substitution rates were estimated in MrBayes v. 3.1.2. Nucleotide frequencies, substitution rates, the shape of the gamma distribution, the proportion of invariable sites, and the overall rate of evolution were allowed to vary among partitions (unlink statefreq = (all) revmat = (all) shape = (all) pinvar = (all)). Four chains of Markov chain Monte Carlo (MCMC) were run for 50 million generations, sampling every 1000 generations. The first 25% of the sampled trees were discarded as burn-in, and the lnL probability plot was checked for stationarity in TRACER v. 1.5 (Rambaut and Drummond, 2007).

Branch support in parsimony was assessed using symmetric jackknife (SJ) resample and partitioned bremer support (PBS) (Baker and DeSalle, 1997; Gatesy et al., 1999) in TNT. The results from SJ are expressed in differences of group frequencies (GC for group present/contradictory; Goloboff et al., 2003) instead of straight group frequencies. Partitioned Bremer support was calculated using a script written by Carlos Peña (pbsup.run at http://www.zmuc.dk/public/phylogeny/tnt/scripts). Posterior probabilities and bootstrap support are provided for the BI and ML trees, respectively. Trees were edited using FigTree v. 1.3.1 (Rambaut, 2006–2009; http://tree.bio.ed.ac.uk/software/figtree) and Adobe Photoshop®.

Results

Molecular partition

DNA markers analysed independently produced many equally parsimonious solutions (results not shown), except for CAD, which produced only three. These solutions differed as to the relative position between groups of species after branching of *H. chloe* and *H. atlantis*. As a result, strict consensus trees were poorly resolved for all markers. Under ML and BI, optimal solutions were characterized by having very short branches between species and between species groups. The samples of six of the eight species with more than one specimen clustered together in all individual gene analyses, except for *H. arinome* and *H. glauconome*, samples of which did not form monophyletic groups even after all the DNA evidence was combined.

Parsimony analysis under EW produced two most parsimonious trees with alternative resolutions between specimens of *H. fornax*. The EIW analysis under values of the concavity constant from k = 7–20 found one optimal tree that was identical to one of the two EW trees. This tree with the relationships within *H. fornax* collapsed is shown in Fig. 3a: numbers above and below branches represent GC values from the SJ resample and the number of nucleotide substitutions.

Parsimony analyses of the DNA partition support the monophyly of *Hamadryas* and split the genera into seven lineages (colour coded in Fig. 3a and thereafter), of which five are species groups and two are single species lineages. *Hamadryas chloe* and *H. atlantis* constitute early splits followed by the *feronia*- and *amphi*-

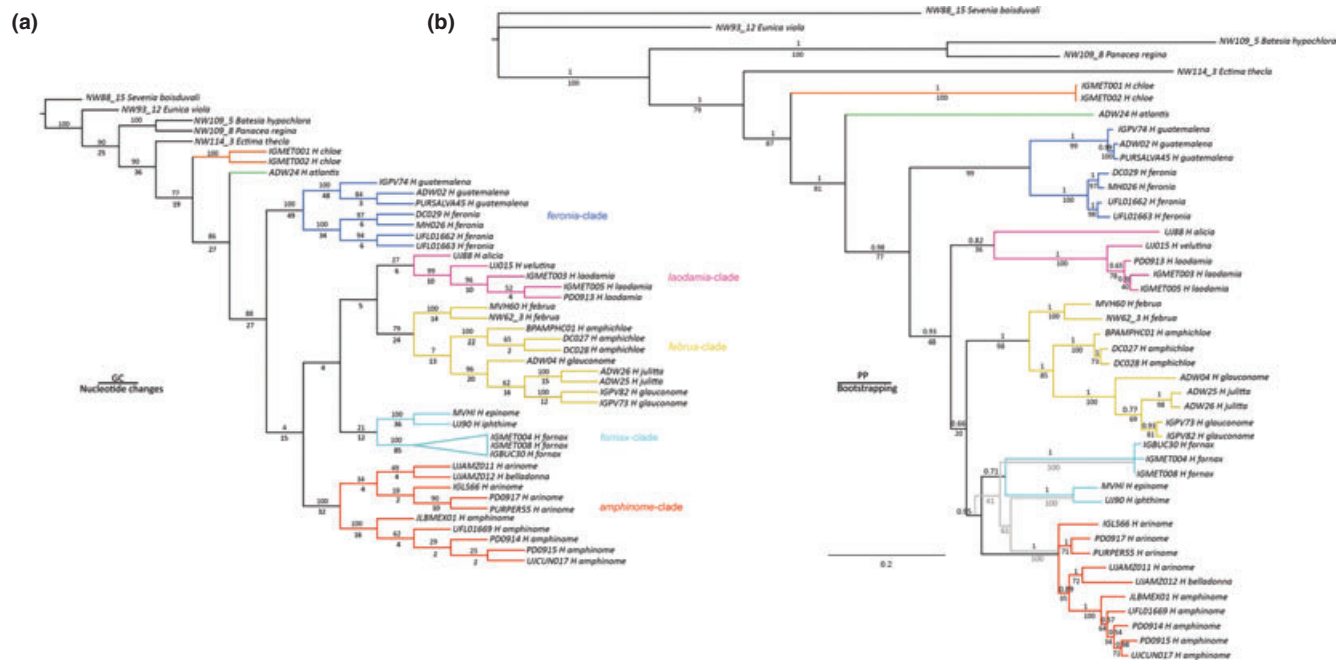

Fig. 3. DNA-based *Hamadryas* phylogeny. (A) Parsimony results; (B) Bayesian inference (BI) and maximum likelihood (ML) analysis (grey inset). Grey branches show an alternative relationship of the *fornax* clade to the *amphinome* clade found under ML (the only difference from the BI tree).

nome clades, and an assemblage including the *fornax*- and *laodamia* + *februa* clades.

Both model-based methods found similar topologies (Fig. 3b), which differed from that recovered by parsimony (Fig. 3a). While BI yielded the same seven lineages supported by parsimony, the ML analysis did not recover the *fornax* clade, and *H. epinome* plus *H. iphthime* grouped with the *amphinome* clade (see grey branches in Fig. 3b). Parsimony and BI topologies differed in the position of the *laodamia* clade, which is sister to the *februa* clade in Fig. 3a but splits off earlier than the *februa* clade in Fig. 3b. The position of the *fornax* clade also differs between these two topologies: it is sister to the *februa* + *laodamia* clades under parsimony (Fig. 3a), but it groups with the *amphinome* clade under BI.

Combined evidence

Parsimony analysis under EW and EIW (with $k > 30$) produced the same optimal topology (Fig. 4). Lower values of the concavity constant (more weight against homoplasy) found a tree similar to Fig. 4, except that *H. fornax* and *H. epinome* + *H. iphthime* are recovered as a clade (grey branches in Fig. 4). BI found a topology slightly different from the one obtained with parsimony, in which *H. fornax*, *H. epinome*, and *H. iphthime* appear as sister clade to the *amphinome* and the *laodamia* clades (Fig. 5).

Under both parsimony and BI, the combined data tree has the same seven lineages recovered by the molecular partition alone (compare Figs 3a with Figs 4 and 5), but excludes *H. alicia* from the *laodamia* clade, splitting *Hamadryas* into eight lineages. Topologies based on the DNA partition and the combined data differed mainly in the position of the *laodamia*- and the *fornax* clades. Based on the DNA partition the *laodamia* clade was either sister to the *februa* clade (parsimony) or branched off earlier, after the *feronia* clade (BI and ML). In contrast, in the combined data tree the *laodamia* clade is sister to the *amphinome* clade. Under parsimony, the combined data generally do not support *H. epinome*, *H. iphthime*, and *H. fornax* as a clade (except for $k < 30$ under EIW). Instead, they suggest that *H. iphthime* and *H. epinome* are more closely related to the *februa* clade than to *H. fornax*.

Examination of the characters supporting the topology in Fig. 4 shows relatively low congruence between datasets. For example, 12 nucleotide substitutions and 5 ambiguous morphological changes support the clade resulting from the exclusion of the *feronia* clade (node 34 in Fig. 4). The sister relationship between the *laodamia* clade and the *amphinome* clade is supported by only four nucleotide substitutions but nine morphological characters (characters 1 : 0, 18 : 0, 24 : 1, 25 : 0, 30 : 2, 32 : 0, 41 : 1, 57 : 0, 90 : 3). The *amphinome* clade is supported by 33 nucleotide substitutions and

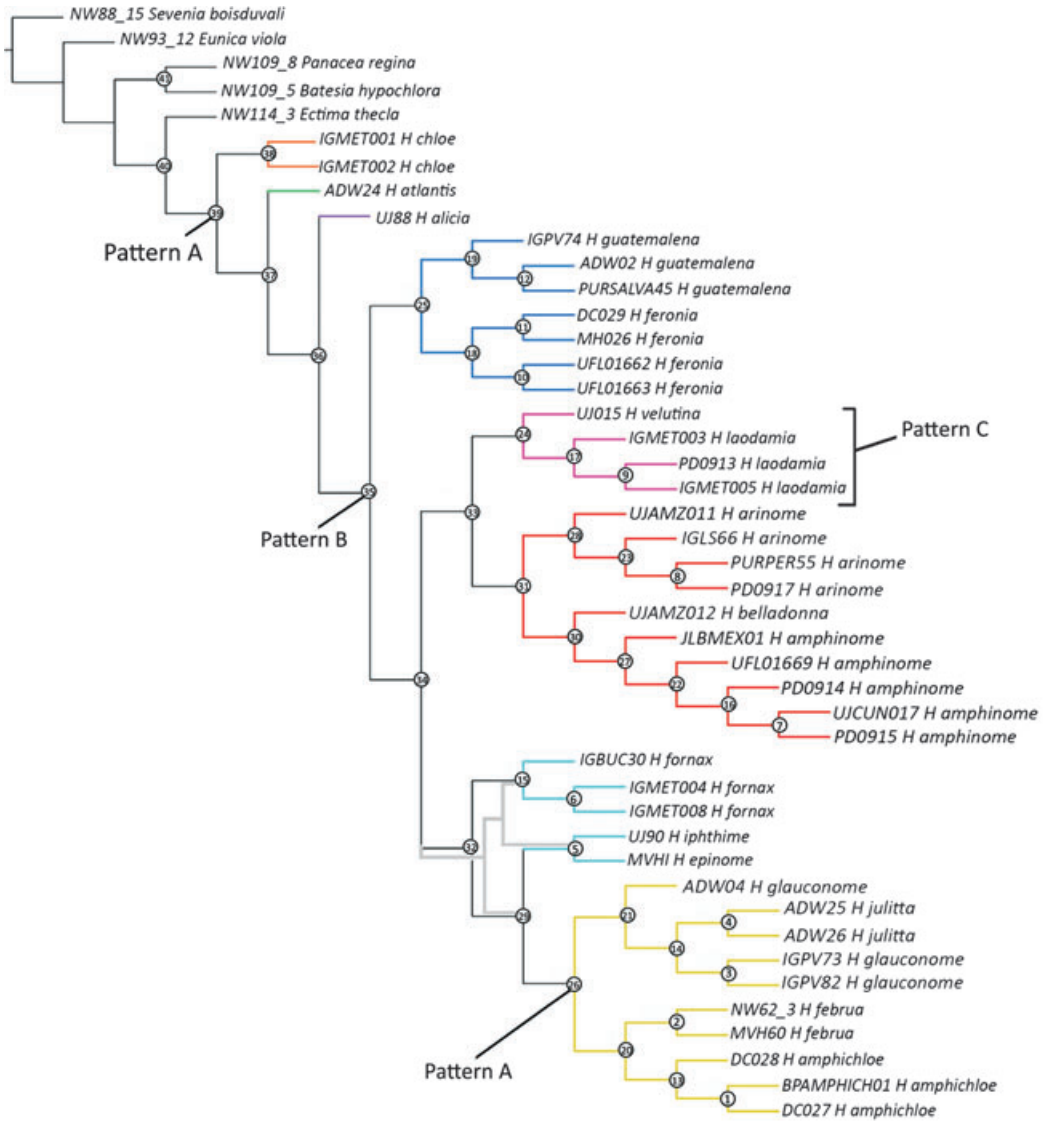

Node	GC	COI	CAD	Ef1a	RPS5	WG	Morph
1	45	0	0	−1	−1	−1	4
2	100	2	10	2	0	1	0
3	100	12	0	−1	0	0	1
4	100	8	3	0	0	0	1
5	100	20	9	0	5	0	0
6	0	15	0	0	0	0	8
7	23	3.5	−2.5	0	−0.2	−1	2.2
8	92	5	−2.7	1.2	−1	0	3.5
9	51	2.5	−0.5	0	0	0	0
10	92	0.5	0	3	0.5	1	0
11	99	0.5	0	3	0.5	1	0
12	87	1	0	0	1	0	0
13	100	7	7	0	0	1	4
14	92	5	−1	−5	−4	1	13
15	100	15	0	0	0	0	8
16	42	3.5	−2.5	0	−0.2	−1	2.2
17	99	7	−1	0	−1	0	3
18	100	9	8	4	1	0	1
19	100	17	0	0	0	0	10
20	0	10	−4	−7	−2.5	−3	7.5
21	97	4	0	0	3	0	0
22	63	1.5	−2.7	0	−0.3	0.5	3
23	46	1	−4	0	0	0	4
24	100	9	1.3	−3.7	−2	−1	24.3
25	100	8	0	0	0	0	9
26	99	−2	2.6	−2	−1.9	−0.7	18.3
27	100	2	1.5	2	2.5	0.5	3.5
28	12	1	−4	0	0	0	4
29	19	4.5	−2	−5.5	−2.5	−1	7.5
30	0	1	−2.3	0	−0.2	0	2.5
31	100	12	6	2	1	0	0
32	0	5.5	−2	−5.5	−3	−1	7
33	27	−6	9	−1	−3	−4	7
34	12	2	6.5	−4	−3	−4	4.5
35	52	0	1.3	−4	−2.5	−1.2	10.5
36	99	−1	9	−1	−3	4	11
37	92	2.5	8.5	−0.5	−2.5	−2	9
38	100	35	0	0	0	0	16
39	97	10	3	−4.5	−2.2	1.5	4
40	97	3	0	6	0	4	0
41	100	0.5	25	18.5	−1.5	2	3.5

Fig. 4. Combined evidence topology found under equal weights (EW) and extended implied weights (EIW) under concavity constant k = 7–50 with venation patterns optimized on the tree. Differences among the trees obtained with parsimony and model-based methods do not affect optimization of the venation patterns. The gray branches represent the solution found in topologies under k values< 30. Group frequency values and partitioned Bremer support for each node are shown in the adjacent table.

four morphological changes (characters 38 : 0, 48 : 2, 68 : 0, 71 : 0). Finally, the *fornax* clade is supported only by molecular data (six nucleotide substitutions; compare Figs 3 and 4). All the morphological characters referenced here and in the following sections are described in Table 3.

Resample values (1000 replicates) of the combined data matrix were generally low. The recovered tree from resample (not shown) resembles Fig. 4 but the relationship between some species groups are collapsed, particularly after the *feronia* clade. One example is the sister relationship between the *februa* clade and the *fornax* clade, which was not recovered after resample. Group frequency values of the recovered groups and PBS values for all the nodes are shown in the table adjacent to Fig. 4. PBS values of RPS5, EF1a, and Wingless showed these markers were either indifferent (18 out 41 PBS values were 0 for EF1a and WG) or were in minor conflict with the signal provided by COI, CAD, and morphology (e.g. PBS values for RPS5 were negative for 21 of 41 nodes). For example, the clade resulting from the exclusion of the *feronia* clade (node 34 in Fig. 4) has positive support from COI, CAD, and morphology, but it is in conflict with the signal provided by the other nuclear markers (Ef1a, RPS5, WG). The sister relationship among the *laodamia* and *amphinome* clades is supported by CAD and morphology, but

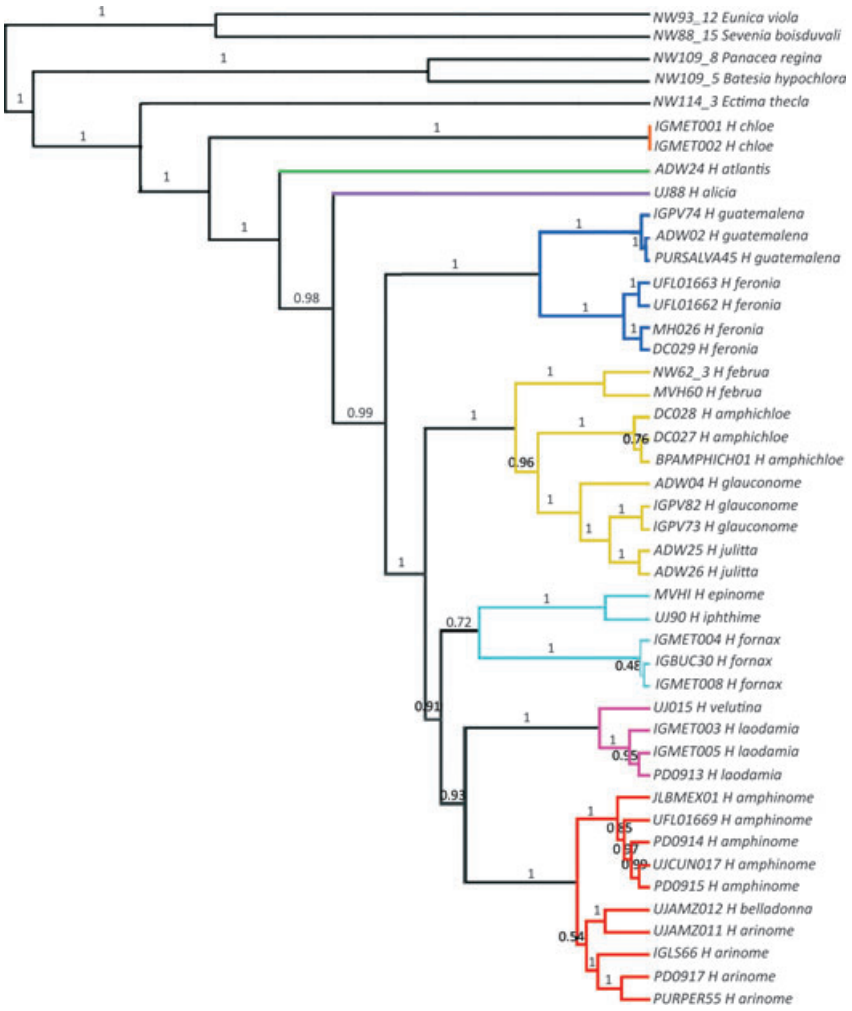

Fig. 5. Majority rule consensus with posterior probabilities above the branches found with MrBayes.

contradicted by other molecular markers (node 33 in Fig. 4). The relationship of *H. fornax*, *H. iphthime*, and *H. epinome* (as a clade or not) with the *februa* clade is supported by COI and morphology only, and is in conflict with the other markers (node 32 in Fig. 4). In contrast, the signal provided by morphology was not in conflict with any of the nodes. Furthermore, CAD agreed with the morphology in 25 of 41 nodes, and in 11 nodes with the signal provided by COI.

The results above prompted the exploratory analyses of two partitions: EF1a + Rps5 + WG and COI + CAD + morphology. The EIW analyses of these partitions found one optimal tree for each. EF1a + Rps5 + WG yielded a tree that resembled the optimal tree obtained using Rps5 alone (not illustrated). In this tree, one of the outgroups (*Ectima thecla*) is the sister group of *H. chloe*, rendering *Hamadryas* paraphyletic. In agreement with the tree based on the combined data (Fig. 4), the next split is *H. atlantis*. The *laodamia* clade is sister to the remaining species, which are divided into two clades: the *februa* clade together with *H. fornax*, *H. iphthime*, and *H. epinome* as a monophyletic group and *amphinome* plus *feronia* clades. Resample of this partition showed that all the relationships among the species groups above the *laodamia* clade collapse after SJ. The tree yielded by COI + CAD + morphology had the same topology obtained with the combined evidence (Fig. 4). The relationships between the *fornax* and *februa* clades do not collapse after resample in the COI + CAD + morphology tree, unlike the combined evidence tree. Overall, the COI + CAD + morphology tree had higher GC values than the combined evidence tree.

Finally, our results point to the need for future taxonomic work. Samples of *H. julitta* fell inside samples of *H. glauconome* in all analyses (Figs 3–5). These results indicate that the species status of *H. julitta* should be re-evaluated.

Table 3
Morphological characters from Garzón-Orduña (2012) referenced in this study

Character	Defintion
1	White scales on antennae: (0) absent, (1) present
3	In males, FW veins R and Rs1 (Jenkins, 1983): (0) separated, (1) sharing a common stem
4	In males, FW Rs − Rs2 + 3 + 4, Rs2 + 3 + 4 − M1, and M1–M2: (0) same width as other veins, (1) fully swollen, (2) thick but not swollen
5	In males, FW vein M1: (0) arising from the same point as Rs2 + 3 + 4; (1) arising at midpoint length between Rs2 + 3 + 4 and M2
6	In males, FW vein M2: (0) midly curved towards M3, (1) conspicuously curved towards M3
7	In males, FW crossvein M2–M3 (Jenkins, 1983): (0) joins the M3CuA1 fork, (1) joins the CuA1-CuA2 crossvein, (2) joins M3
18	Ventral coloration of thorax: (0) red, (1) mustard, (2) brown, (3) flax, (4) chalk
22	Spot of blue scales in the proximal portion of the DFW band between elements c and d: (0) absent, (1) present
24	In females, colour of DFW discal cell band between pattern element d and e: (0) white, (1) blue, (2) iridescent green, (3) beige/light brown
25	In females, DFW pattern element e: (0) composed of dark scales, (1) composed of (brown) light scales, (2) composed of blue, (3) composed of red scales
30	DFW in females, width of space between margin of the discal cell and m1–m2 band: (0) narrow, (1) wide, (2) no space, reaching distal margin of discal cell
32	DFW in M2 cell in females, shape of band distal to pattern element e: (0) entire, elongated towards distal margin of wing and pattern element f not visible, (1) split by pattern element f, proximal band oval
35	DHW in females, pattern element d: (0) centre of element d composed of light scales, (1) element d composed of dark scales only, (2) centre of element d composed of red scales
36	DHW in females, colour of the distal edge of discal cell (pattern element e): (0) red, (1) light, (2) dark brown
41	DHW pattern element h (border ocelli): (0) with internal ring, (1) without internal ring
45	Composition of DHW ocellus 2 (Rs cell): (0) complete ocellus, (1) blurred ocellus, (2) only the most external ring present (empty ocellus), (3) external ring and a pupil present, (4) pupil only
56	Location of macrochaete setae on hypandrium: (0) present only at the base of rami, (1) present on lateroposterior margin and some setae reaching the posterior margin of the sternite
57	Macrochaete setae at the posterior margin of hypandrium (base of rami): (0) as long as the macrochaete at the tip of rami, (1) smaller
58	Setae on lateral surface of rami: (0) absent, (1) present but few, (2) present in large numbers
62	In dorsal view, anterior edge of tegumen: (0) appoximately squared, (1) rounded, (2) elongated
90	Shape of ductus bursae: (0) short and wide, (1) rounded, (2) cone shaped (narrow near ductus bursa), (3) pear-shaped

Discussion

DNA versus morphology

Analyses of DNA alone supported the monophyly of *Hamadryas* as well as most of the sister-level relationships inferred with morphology (Fig. 2). Analysed independently, both sources of data support the phylogenetic affinities of *H. februa* with *H. amphichloe* and *H. glauconome*; the sister relationship of *H. feronia* and *H. guatemalena*; and the phylogenetic affinities between *H. laodamia* and *H. velutina* (*H. arete* was not included in the molecular analysis). DNA also provided support for relationships not recovered by morphology, such as *H. amphinome*, *H. arinome*, and *H. belladonna* as a monophyletic group, and *H. iphthime* and *H. epinome* as sister taxa.

The placement of some species was incongruent between datasets. For example, in contrast to morphology, DNA supported *H. chloe* and not *H. atlantis* as the first split within *Hamadryas*. Although DNA places *H. alicia* as sister species of *H. laodamia* and relatives, this placement is based only on an incomplete COI fragment. There are other important discrepancies between both datasets, mainly involving the relative relationships between species groups. Based on morphology, *H. feronia* and *H. guatemalena* are derived species nested within a clade that includes all the species that have some or all the venation components required for sound production (Fig. 2; Garzón-Orduña, 2012). This placement of *H. feronia* and *H. guatemalena* was supported by one morphological synapomorphy (character 22 : 2) and four homoplastic transformations (characters 35 : 1, 36 : 2, 45 : 2, 56 : 1), four of these were colour characters and one regarded the location of macrochaeta in the hypandrium (character 56; Garzón-Orduña, 2012). In contrast, DNA places *H. feronia* and *H. guatemalena* as the first split after *H. atlantis*, an earlier origin than what is implied by morphology. This result was obtained in all the analyses that include all the DNA data, and in the RPS5 and CAD gene trees.

DNA and morphology also disagreed with regard to the relationships among some species groups. The molecular partition did not support a close relationship between *H. amphinome* and relatives plus *H. laodamia* and relatives. This clade was supported in the morphological phylogeny by five apomorphies (charac-

ters 20 : 2, 24 : 1, 45 : 3, 54 : 1, 90 : 3) and six homoplastic transformations (1 : 0, 25 : 0, 30 : 2, 32 : 0, 49 : 2, 60 : 0) and had high resample values (Garzón-Orduña, 2012). Instead, DNA data suggested two alternative positions of the clade of *H. laodamia* and *H. velutina* (depending on whether parsimony or model-based methods are used), neither of which is congruent with morphology alone (Garzón-Orduña, 2012 and Fig. 2).

The molecular partition was moderately sensitive to the perturbations made with resampling. Resample values for the relationships between species groups were intermediate to low, particularly in the case of short internal branches (Fig. 3b). The morphological study also yielded low resample values between species groups (Garzón-Orduña, 2012). Short internal branches of a DNA-based tree and scarce character support of a morphology-based tree are an indication of little divergence between clades and could be a result of rapid speciation (Ober and Heider, 2010). It is therefore evident that neither dataset alone provides robust phylogenetic signal for deeper nodes of the *Hamadryas* tree.

Combined evidence

This study provides a fully resolved species-level phylogenetic hypothesis for *Hamadryas* based on the combination of all available characters (Fig. 4). We favour the phylogenetic hypothesis provided under parsimony because it increases the number of similarities that can be explained by common ancestry, hence increasing the explanatory power of the tree. Furthermore, unlike model-based methods, parsimony trees maintain a direct relationship to the data (Farris, 1983). Two important and unexpected findings of our study are: (i) *H. feronia* and *H. guatemalena* appeared more basal in comparison to the position suggested by morphology, and the combined data suggest these two species constitute a sister group to the rest of *Hamadryas* after the split of *H. alicia*; and (ii) *H. februa* and relatives are nested within a clade of sound-producing *Hamadryas* implying a loss of sound production in this species group.

Although well resolved, short branches of the combined data tree have low support, and these correspond to relationships among species groups within the genus. In particular, it is uncertain whether *H. fornax*, *H. iphthime*, and *H. epinome* form a monophyletic group and whether they are sister taxa to *H. februa* and relatives, or to the *amphinome* plus *laodamia* clade. The result under which *H. fornax*, *H. iphthime*, and *H. epinome* are sister to *februa* and relatives was obtained only under parsimony and it was lost after resampling; meanwhile BI and EIW with low values of the concavity constant (penalizing homoplasy harder) suggest these species are sister to the *amphinome* plus *laodamia* clade. The absence of resampling support in parsimony suggests that their position might change with the addition of more data. Similarly to other species-level phylogenetic studies on butterflies, this study found low support at the intermediate parts of the tree, while obtaining strong support for clades near the tips (Monteiro and Pierce, 2001; Silva Brandão et al., 2008).

Partitioned Bremer support showed interesting trends in the interaction between mitochondrial and nuclear DNA markers. The PBS results, although with low negative values, showed that three (WG, Rps5, Ef1a) of the four nuclear markers were in conflict with the combined evidence tree, mainly at the nodes that were supported by COI and morphology; the exception was CAD, which was in agreement with COI and morphology in several of these same nodes. Exploratory analysis of these partitions (WG + Rps5 + Ef1a versus COI + CAD + morphology) showed that the conflict stands from each partition, suggesting a rather different phylogenetic history of *Hamadryas*. The signal provided by WG + Rps5 + Ef1a is evidently not enough to support a monophyletic origin of *Hamadryas* (which has never been questioned). Furthermore, most of the relationships supported by these genes collapsed after resample, suggesting there is additional internal conflict between the three markers. Overall, the analysis of COI + CAD + morphology confirmed that the tree provided in this paper combining all the evidence is the best hypothesis of the phylogenetic relationships of *Hamadryas* to date.

Wahlberg et al. (2009) found strong conflict between the signal provided by mitochondrial (COI and ND1) and nuclear markers (EF1-a, WG, GAPDH, RPS5). Our results are in agreement with their findings even though that study did not include CAD. Minor incongruence between mitochondrial and nuclear DNA markers could be the resultant signature of recent divergence, in which case slowly evolving genes have not had enough time to sort (McCracken and Sorenson, 2005). As mentioned in the results, single gene reconstructions of these markers show low resolution, suggesting ambiguity in the data in concordance with incomplete lineage sorting.

In contrast, seemingly ambiguous or contradictory datasets can produce a robust phylogenetic signal upon their combination (Miller et al., 1997). This is due to the interaction between characters, and is known as "hidden support" (Gatesy et al., 1999). In our study, for example, DNA-based analyses suggested that the *laodamia* clade was closely related to the *februa* clade. Yet EW, EIW, and BI analyses of the combined evidence supported the relationships suggested by morphology alone: that *H. laodamia* and relatives are a sister clade to *H. amphinome* and relatives

(although they did not form a monophyletic group based on morphology). The emergence of this relationship on the combination of datasets shows that both the molecular and morphological partitions contained signal, supporting a clade including *laodamia*, *amphinome* and their relatives (see PBS in node 33 of Fig. 4).

Together, the conflict among mitochondrial and nuclear markers, the presence of short internal branches in the combined analyses, and the lack of morphological characters supporting relationships between species groups seem to suggest that some clades in *Hamadryas* diverged rapidly. Limitations to the current phylogenetic hypothesis of *Hamadryas* could be addressed by using longer fragments and other fast-evolving genes, as well as completing the sequences for species containing missing entries, as in the case of *H. alicia* in this study.

Implications for the evolution of sound production

In *Hamadryas*, males that are known to produce sound exhibit five modifications of the FW venation (Fig. 1B). The modifications are: (i) R1 and R2 veins stalked (character 3 : 1 in Garzón-Orduña, 2012); (ii) M1 rising independently from R3, R4–R5 (character 5 : 1); (iii) M2 conspicuously bowed (character 6 : 1); (iv) cross-vein at posterior edge of discal cell swollen (character 4 : 1); (v) M2–M3 cross-vein joins cu1–cu2 cross-vein (character 7 : 1).

Trees based on the combined data (parsimony and Bayesian) suggest a different scenario (Fig. 4) for the evolution of sound production from that suggested by morphology alone (Fig. 2; Garzón-Orduña, 2012). Based on combined data, these five changes in venation appear earlier in the phylogeny (compare Fig. 4 with Fig. 2; Garzón-Orduña, 2012). Here, however, the venation for sound production is inferred to have evolved after *H. alicia* branched off, at the common ancestor of *H. feronia* plus *H. guatemalena* and the rest of *Hamadryas* (B in Fig. 4). More importantly, the tree based on combined data suggests two losses of the venation required for sound production: one in which the five characters reverse at the node of *H. februa* and relatives (a complete reversal to the plesiomorphic venation; A in Fig. 4) and another in which only two of the five characters reverse at the node of the *laodamia* clade (resulting in an intermediate venation pattern; C in Fig. 4).

Although both reversals imply the loss of sound production, they are different. Males of *H. laodamia* and *H. velutina* show two venation character reversals: FW vein M_2 is almost straight (6 : 0), and the cross-vein at the posterior edge of the discal cell is thicker than in other species but not swollen (4 : 2). The loss of sound production in these species concurred with the evolution of scent scales (androconia) and sexual dimorphism (SD), which has been interpreted as a switch in sexual recognition signals, from sound to visual and scent cues (Garzón-Orduña, 2012). The loss of sound production in the clade of *H. februa* and relatives is more difficult to explain because it implies the reversal of all five characters. Based on field observations of interactions between sound-producing males and females of *H. feronia*, Otero (1988) concluded that spiral flights seem to have little importance in the sexual recognition of this species; this is in stark contrast to the interactions of *H. februa*, in which spiral flights are the signature response of males to chases during aerial interactions (Otero, 1988; D. Otero, pers. commun.).

The presence of an intermediate venation in a clade that does not produce sounds, *H. laodamia* and relatives, suggests that changes in characters 6 and/or 4 are critical to the production of sound. Otero's (1990) ablation experiments on *H. feronia* showed that if the cross-vein at the apical part of the discal cell is removed, sound production ceases. His experiment, although extreme, represents the only available analogy between states 0 and 1 of character 4, and highlights the importance of this character for the production of sound.

As stated above, neither *H. februa* nor any of the members of the *februa* clade have the venation components for sound production. However, there are some accounts about the ability of *H. februa* to produce sound. Several authors reported sound production in populations of *H. februa* from Brazil (Jenkins, 1983), Costa Rica (DeVries, 1983; Monge-Nájera and Hernández, 1991), El Salvador (Muyshondt and Muyshondt, 1975b), and Mexico (Ross, 1963). In contrast, Otero (1988) and Marini-Filho and Benson (2010) tested (based on hand tests and in field cages) the ability of *H. februa* to make sound in populations from Venezuela and from Brazil, respectively, and found that none of the specimens studied was capable of producing sound. Given the results of this study, the incongruence between these accounts is intriguing; the existence of cryptic species or sound-production polymorphism via an additional (unknown) mechanism of sound production cannot be discounted.

Acknowledgements

For the donation of samples we are deeply thankful to Giovanny Fagua, Monica Higuera, Diana Caballero, Malva Hernandez, Andy Warren, Peter Boyer, Keith Willmott, Phil DeVries, and Geoff Gallice. Many thanks to Pablo Goloboff and J. Salvador Arias for their comments on the manuscript and discussion of cladistics methods. We are thankful to the Lepidoptera Research Foundation, the Organization for Tropi-

cal Studies (OTS), the Department of Biological Sciences (University of New Orleans), and the Office of Latin American Studies at the University of New Orleans for funding for this study. I.J.G.O. is deeply thankful to Lyndon Coghill, Johel Chaves, and Jerome Murienne for their assistance throughout the molecular work involved in this study.

References

Baker, R.H., DeSalle, R., 1997. Multiple sources of character information and the information and the phylogeny of Hawaiian drosophilids. Syst. Biol. 46, 654–673.

Baker, R., Gatesy, J., 2002. Is morphology still relevant? In: DeSalle, R., Wheeler, W., Giribet, G. (Eds.), Molecular Systematics and Evolution: Theory and Practice. Birkhauser Verlag, Basel, pp. 163–174.

Brower, A.V.Z., DeSalle, R., 1998. Patterns of mitochondrial versus nuclear DNA sequence divergence among nymphalid butterflies: the utility of *wingless* as a source of characters for phylogenetic inference. Insect Mol. Biol. 7, 1–10.

Cho, S., Mitchell, A., Regier, J.C., Mitter, C., Poole, R.W., Friedlander, T.P., Zhao, S., 1995. A highly conserved nuclear gene for low level phylogenetics: elongation factor 1-alpha recovers morphology-based tree for heliothine moths. Mol. Biol. Evol. 12, 650–656.

Darriba, D., Taboada, G.L., Doallo, R., Posada, D., 2012. jModelTest 2: more models, new heuristics and parallel computing. Nat. Methods 9, 772.

DeVries, P.J., 1983. *Hamadryas februa* (Nymphalidae). In: Janzen, D.H. (ed.) Costa Rican Natural History. University of Chicago Press, Chicago, IL. pp. 729–730.

DeVries, P.J., 1987. Butterflies of Costa Rica: and Their Natural History. Vol. 1: Papilionidae, Pieridae, Nymphalidae. Princeton University Press, Princeton.

Drummond, A.J., Ashton, B., Buxton, S., Cheung, M., Cooper, A., Duran, C., Field, M., Heled, J., Kearse, M., Markowitz, S., Moir, R., Stones-Havas, S., Sturrock, S., Thierer, T., Wilson, A., 2011. Geneious v5.4. Available from http://www.geneious.com/

Edgar, R.C., 2004. MUSCLE: multiple sequence alignment with high accuracy and high throughput. Nucleic Acids Res. 32, 1792–1797.

Farris, J.S., 1983. The logical basis of phylogenetic analysis. In: Platnick, N.I., Funk, V.A. (Eds.), Advances in Cladistics, Volume 2, Proceedings of the Second Meeting of the Willi Hennig Society. Columbia University Press, New York, pp. 1–47.

Farris, J.S., Kallersjo, M., Kluge, A.G., Bult, C., 1994a. Testing the significance of incongruence. Cladistics, 10, 315–319.

Folmer, O., Black, M., Hoeh, W., Lutz, R., Vrijenhoek, R., 1994. DNA primers for amplification of mitochondrial cytochrome c oxidase subunit I from diverse metazoan invertebrates. Mol. Mar. Biol. Biotech. 3, 294–299.

Fruhstorfer, H., 1916. 54. Genus *Ageronia*. In: Seitz, A. (Ed.), Macrolepidoptera of the World, Vol. 5. Alfred Kernen, Stuttgart, pp. 537–545.

Garzón-Orduña, I.J., 2012. Phylogenetic evidence for loss of sound production and a shift in sexual recognition signals in *Hamadryas* butterflies (Nymphalidae: Biblidinae). Syst. Entomol. 37, 84–101.

Gatesy, J., O'Grady, P., Baker, R.H., 1999. Corroboration among data sets in simultaneous analysis: hidden support for phylogenetic relationships among higher level artiodactyl taxa. Cladistics, 15, 271–313.

Giannini, N.P., Simmons, N.B., 2005. Conflict and congruence in a combined DNA-morphology analysis of megachiropteran bat relationships (Mammalia: Chiroptera: Pteropodidae). Cladistics, 21, 411–437.

Godman, F.D., Salvin, O., 1883. Biologia Centrali-Americana Rhopalocera. 1, 265–288.

Goloboff, P.A., Farris, J.S., Källersjö, M., Oxelman, B., Ramírez, M.J., Szumik, C.A., 2003. Improvements to resampling measures of group support. Cladistics, 19, 324–332.

Goloboff, P.A., Farris, J., Nixon, K., 2008. TNT a free program for phylogenetic analysis. Cladistics, 24, 774–786.

Huelsenbeck, J.P., Ronquist, F., 2001. MRBAYES: Bayesian inference of phylogeny. Bioinformatics, 17, 754–755.

Jenkins, D.W., 1983. Neotropical Nymphalidae I. Revision of *Hamadryas*. Bull. Allyn Museum, 81, 146 pp.

Jiggins, C.D., Mallarino, R., Willmott, K.R., Bermingham, E., 2006. The phylogenetic pattern of speciation and wing pattern change in Neotropical *Ithomia* butterflies (Lepidoptera: Nymphalidae). Evolution, 60, 1454–1466.

Kluge, A., 1989. A concern for evidence and a phylogenetic hypothesis of relationships among *Epicrates* (Boidae, Serpentes). Syst. Zool. 38, 7–25.

Lamas, G., 2004. Biblidinae. Atlas of Neotropical Lepidoptera (ed. by J.B. Heppner), Checklist: Part 4A Hesperioidea-Papilionoidea. (ed. by G. Lamas), 234–247. Association of Tropical Lepidoptera/ Scientific Publishers, Gainesville, Florida.

Lewis, P.O., 2001. A likelihood approach to estimating phylogeny from discrete morphological character data. Syst. Biol. 50, 913–925.

Lopardo, L., Giribert, G., Hormiga, G., 2011. Morphology to the rescue: molecular data and the signal of morphological characters in combined phylogenetic analyses—a case study from mysmenid spider (Araneae, Mysmenidae), with comments on the evolution of web architecture. Cladistics, 27, 278–330.

Marini-Filho, O.J., Benson, W.W., 2010. Use of percussion and aerial chases in sexual recognition in Neotropical *Hamadryas* butterflies (Nymphalidae). J. Res. Lepid. 42, 5–12.

McCracken, K.G., Sorenson, M.D., 2005. Is homoplasy or lineage sorting the source of incongruent mtDNA and nuclear gene trees in the stiff-tailed ducks (*Nomonyx-Oxyura*)? Syst. Biol. 54, 35–55.

Mickevich, M.F., Farris, J.S., 1981. The implications of congruence in *Menidia*. Syst. Zool. 30, 351–370.

Miller, J.S., Brower, A.V.Z., De Salle, R., 1997. Phylogeny of the Neotropic moth tribe *Josiini* (Notodontidae: Dioptinae): comparing and combining evidence from DNA sequences and morphology. Biol. J. Linn. Soc. 60, 297–316.

Monge-Nájera, J., Hernández, F., 1991. A morphological search for the sound mechanism of *Hamadryas* butterflies (Lepidoptera: Nymphalidae). J. Res. Lepid. 30, 196–208.

Monteiro, A., Pierce, N., 2001. Phylogeny of *Bicyclus* (Lepidoptera: Nymphalidae) inferred from COI, COII and EF1a gene sequences. Mol. Phyl. Evol. 18, 264–281.

Muyshondt, A., Muyshondt, A.J., 1975a. Notes on the life cycle and natural history of butterflies of El Salvador. IIIB. *Hamadryas amphinome* L. (Nymphalidae–Hamadryadinae). J. N.Y. Entomol. Soc., LXXXIII, 181–191.

Muyshondt, A., Muyshondt, A.J., 1975b. Notes on the life cycle and natural history of Butterflies of El Salvador. IB. *Hamadryas februa* (Nymphalidae–Hamadryadinae). N.Y. Entomol. Soc., LXXXIII, 157–169.

Nixon, K.C., 1999. The parsimony ratchet, a new method for rapid parsimony analysis. Cladistics, 15, 407–414.

Nixon, K.C., Carpenter, J.M., 1996. On simultaneous analysis. Cladistics, 12, 221–241.

Nylin, S., Nyblom, K., Ronquist, F., Janz, N., Belicek, J., Källersjö, M., 2001. Phylogeny of *Polygonia*, *Nymphalis* and related butterflies (Lepidoptera: Nymphalidae): a total evidence analysis. Biol. J. Linn. Soc. 132, 441–468.

Ober, K.A., Heider, T.N., 2010. Phylogenetic diversification patterns and divergence times in ground beetles (Coleoptera: Carabidae: Harpalinae). BMC Evol. Biol. 10, 262.

Otero, D., 1988. Contribución a la Historia Natural del Genero *Hamadryas* (Lepidoptera: Nymphalidae). Departamento e instituto de zoologia agrícola, Facultad de Agronomia, Universidad Central de Venezuela, Maracay.

Otero, D., 1990. Estudio de algunos caracteres para su uso en la clasificación de Eurytelinae (Lepidoptera: Nymphalidae). Bol. Entomol. Venez. 5, 123–138.

Penz, C., DeVries, P.J., Wahlberg, N., 2012. Diversification of *Morpho* butterflies (Lepidoptera, Nymphalidae): a re-evaluation of morphological characters and new insight from DNA sequence. Syst. Entomol. 37, 670–685.

Rambaut, A., Drummond, A.J., 2007. Tracer v1.5. Available at http://beast.bio.ed.ac.uk/Tracer. Accessed 2012 January.

Ross, G.N., 1963. Evidence for lack of territoriality in two species of *Hamadryas*, Nymphalidae. J. Res. Lepid. 3, 207–229.

Silva Brandão, K.L., Wahlberg, N., Francini, R.B., Azeredo-Espin, A.M.L., Brown, K.S. Jr, Paluch, M., Lees, D.C., Freitas, A.V.L., 2008. Phylogenetic relationships of butterflies of the tribe Acraeini (Lepidoptera, Nymphalidae, Heliconiinae) and the evolution of host plant use. Mol. Phyl. Evol. 46, 515–531.

Simon, C., Frati, F., Beckenbach, A., Crespi, B., Liu, H., Flook, P., 1994. Evolution, weighting and phylogenetic utility of mitochondrial gene sequences and a compilation of conserved polymerase chain reaction primers. Ann. Entomol. Soc. Am. 87, 651–701.

Stamatakis, A., Hoover, P., Rougemont, J., 2008. A rapid bootstrap algorithm for the RAxML web servers. Syst. Biol. 57, 758–771.

Vaidya, G., Lohman, D.J., Meier, R., 2011. SequenceMatrix: concatenation software for the fast assembly of multi-gene datasets with character set and codon information. Cladistics, 27, 171–180.

Wahlberg, N., Nylin, S., 2003. Morphology versus molecules: resolution of the positions of *Nymphalis*, *Polygonia* and related genera (Lepidoptera: Nymphalidae). Cladistics, 19, 213–223.

Wahlberg, N., Wheat, C.W., 2008. Genomics outputs serve the phylogenomic pioneers: designing novel nuclear markers for genomic DNA extractions of Lepidoptera. Syst. Biol. 57, 231–242.

Wahlberg, N., Braby, M.F., Brower, A.V.Z., de Jong, R.M., Lee, M., Nylin, S., Pierce, N., Sperling, F.A., Vila, R., Warren, A.D., Zakharov, E., 2005. Synergistic effects of combining morphological and molecular data in resolving the phylogeny of butterflies and skippers. Proc. R. Soc. B 272, 1577–1586.

Wahlberg, N., Weingartner, E., Warren, A.D., Nylin, S., 2009. Timing major conflict between mitochondrial and nuclear genes in species relationships of *Polygonia* butterflies (Nymphalidae: Nymphalini). BMC Evol. Biol. 9, 92.

Yack, J., Otero, L.D., Dawson, J.D., Surlykke, A., Fullard, J.H., 2000. Sound production and hearing in the blue cracker butterfly *Hamadryas feronia* (Lepidoptera, Nymphalidae) from Venezuela. J. Exp. Biol. 203, 3689–3702.